THE JOURNAL OF BIOLOGICAL CHEMISTRY VOL. 287, NO. 1, pp. 152–163, January 4, 2013

Sorting Nexin 1 Loss Results in D_5 Dopamine Receptor Dysfunction in Human Renal Proximal Tubule Cells and Hypertension in Mice*

Received for publication, October 16, 2012, and in revised form, November 13, 2012 Published, JBC Papers in Press, November 14, 2012, DOI 10.1074/jbc.M112.428458

Van Anthony M. Villar[‡1,2], John Edward Jones[‡1], Ines Armando[‡1], Laureano D. Asico[‡1], Crisanto S. Escano, Jr.[‡1], Hewang Lee[‡1], Xiaoyan Wang[‡1], Yu Yang[‡1], Annabelle M. Pascua-Crusan[‡1], Cynthia P. Palmes-Saloma[§], Robin A. Felder[¶], and Pedro A. Jose[‡1]

From the [‡]Center for Molecular Physiology Research, Children's Research Institute, Children's National Medical Center, Washington D. C. 20010, [§]National Institute of Molecular Biology and Biotechnology, University of the Philippines, Diliman, Quezon City, Philippines 1101, and the [¶]Department of Pathology, The University of Virginia School of Medicine, Charlottesville, Virginia 22908

Background: SNX1 is a protein involved in the trafficking of internalized receptors.
Results: Inhibition of SNX1 expression leads to failure of D_5R endocytosis and signaling.
Conclusion: Depletion SNX1 function results in D_5R dysfunction and high blood pressure.
Significance: Loss of SNX1 expression may be a novel mechanism for the development of hypertension.

The peripheral dopaminergic system plays a crucial role in blood pressure regulation through its actions on renal hemodynamics and epithelial ion transport. The dopamine D5 receptor (D_5R) interacts with sorting nexin 1 (SNX1), a protein involved in receptor retrieval from the trans-Golgi network. In this report, we elucidated the spatial, temporal, and functional significance of this interaction in human renal proximal tubule cells and HEK293 cells stably expressing human D_5R and in mice. Silencing of SNX1 expression via RNAi resulted in the failure of D_5R to internalize and bind GTP, blunting of the agonist-induced increase in cAMP production and decrease in sodium transport, and up-regulation of angiotensin II receptor expression, of which expression was previously shown to be negatively regulated by D_5R. Moreover, siRNA-mediated depletion of renal SNX1 in C57BL/6J and BALB/cJ mice resulted in increased blood pressure and blunted natriuretic response to agonist in salt-loaded BALB/cJ mice. These data demonstrate a crucial role for SNX1 in D_5R trafficking and that SNX1 depletion results in D_5R dysfunction and thus may represent a novel mechanism for the pathogenesis of essential hypertension.

The peripheral dopaminergic system plays an important role in blood pressure regulation through its actions on renal hemodynamics and epithelial ion transport (1–3). Peripherally, dopamine acts through its cognate cell surface receptors in adrenergic nerve endings, blood vessels, and epithelial tissues, including those in the kidneys and intestines (1, 2, 4). Under conditions of moderate sodium excess, dopamine generated by renal proximal tubule cells acts on renal tubular cells to decrease sodium transport by at least 50% (1, 2, 5), an effect exerted mainly through the D_1-like receptors (6, 7). The dopamine receptors belong to the rhodopsin-like family of G-protein-coupled receptors (GPCRs)[3] and are classified structurally and pharmacologically into D_1-like (D_1R and D_5R) and D_2-like receptors (D_2R, D_3R, and D_4R) (8, 9).

In human essential hypertension and in some rodent models of genetic hypertension, dopamine fails to elicit an appropriate renal autocrine/paracrine response that results in a loss of inhibition of several sodium transport mechanisms and decreased renal sodium excretion (1, 2, 10, 11). Inactivation of any of the dopamine receptors in mice results in hypertension, thus demonstrating the important role of these receptors in the regulation of blood pressure (12–14). In particular, deletion of the D_5R results in salt sensitivity and increased blood pressure (12, 15).

Ligand binding by GPCRs, including the D_5R, results in the rapid desensitization (waning of receptor responsiveness to further stimulation) through a change in receptor conformation, dissociation from its G protein, modification and/or phosphorylation by GPCR kinases (GRK, G protein-coupled receptor kinases), and receptor endocytosis. In general, the internalized GPCRs undergo vectorial yet dichotomous pathways of dephosphorylation (resensitization), recycling, and reinsertion into the cell membrane or, alternatively, degradation via the lysosome or proteasome. Proper receptor internalization and sorting are highly regulated to ensure the accuracy of the intracellular signal and to limit the specificity and extent

* This work was supported, in whole or in part, by National Institutes of Health Grants HL68686, HL23081, HL074940, HL092196, and DK39308 and awards UL1RR031988 and KL2 RR031987 (National Institutes of Health National Center for Research Resources). This work was also supported by the Lombardi Comprehensive Cancer Center Microscopy and Imaging Shared Resource and United States Public Health Service Grants 2P30-CA-51008 and 1S10 RR15768-01.

[1] Present address: Dept. of Medicine, University of Maryland School of Medicine, Baltimore, MD 21201.

[2] To whom correspondence should be addressed: Division of Nephrology, Dept. of Medicine, University of Maryland School of Medicine, 20 Penn St., Suite S003C, Baltimore, MD 21201. Tel.: 410-706-6014; Fax: 410-706-6034; E-mail: vvillar@medicine.umaryland.edu.

[3] The abbreviations used are: GPCR, G protein-coupled receptor; AT_1R, angiotensin II type 1 receptor; D_1R, dopamine D_1 receptor; D_5R, dopamine D_5 receptor; hPTC, human renal proximal tubule cell; SNX1, sorting nexin 1; SHR, spontaneously hypertensive rat; Ab, antibody; GTP-Eu, GTP-europium; ANOVA, analysis of variance; UNaV, urinary sodium excretion.

of cellular response. The D_5R undergoes both homologous and heterologous endocytosis that is clathrin- and dynamin-dependent but may be arrestin-independent followed by receptor recycling (16). The sorting and trafficking of GPCRs appear to be mediated by the sorting nexins (17) among other proteins. The cytoplasmic tail of D_5R was shown to strongly interact with sorting nexin 1 (SNX1) (18).

The sorting nexin family comprises a diverse group of cytoplasmic and membrane-associated proteins that are involved in post-endocytic receptor trafficking and contain the canonical PX domain that targets and binds phosphatidylinositides (19). SNX1 is the ortholog of the yeast VPS5p that is involved in vacuolar trans-Golgi network trafficking of proteins. It is distributed in both the plasma membrane and cytosol, where it exists in complex with other proteins (20). SNX1 homodimerizes or heterodimerizes with SNX2, resulting in the membrane-targeting component of the mammalian retromer (21), which is a complex of several proteins that is involved in the retrograde trafficking between early endosomes and the *trans*-Golgi network. SNX1 is involved in the retrograde sorting of several receptors, such as the EGF receptor (22, 23), sortillin, and the mannose 6-phosphate receptor (24). Independent of its retromer function, SNX1 has been shown to promote the lysosomal degradation of protease-activated receptor 1 (PAR1) (25), modulate Kalirin-7/Duo- and RhoG-dependent actin remodeling in epithelial cells (26), and direct the ADP $P2Y_1$ receptor into the slow recycling pathway (27).

In this study we established the temporal, spatial, and physiological significance of the interaction between the D_5R and SNX1. Our results show that in human renal proximal tubule cells (hPTCs) and human embryonic kidney (HEK293) cells heterologously expressing human D_5R (HEK293-hD_5R), the interaction of both proteins is essential for the trafficking and function of the receptor. Alterations in this interaction result in D_5R dysfunction and high blood pressure in mice and hence may be one of the underlying mechanisms in essential hypertension.

EXPERIMENTAL PROCEDURES

Cell Lines and Cell Culture—Immortalized hPTCs were obtained from normotensive Caucasian males (28, 29). The cells were maintained in DMEM/F-12 (Invitrogen) supplemented with 10% FBS, EGF (10 ng/ml), insulin, transferrin, and selenium mixture (5 μg/ml each) and dexamethasone (4 ng/μl) incubated at 37 °C incubator with humidified 5% CO_2 in 95% air. Immortalized proximal tubule cells from WKY and spontaneously hypertensive rat (SHR) cells were grown in media used for hPTCs (30). HEK293-hD_5R were cultured in DMEM medium supplemented with 10% FBS (13). The cell lines were incubated in serum-free medium for at least 1 h before each treatment. Cells used were limited to those with low passage numbers ($<$25 for hPTCs and $<$40 for HEK293-hD_5R and WKY and SHR proximal tubule cells) to avoid the confounding effects of cellular senescence. The cells tested negative for mycoplasma infection.

Animal Care—All animals used in this study were bred and maintained at the animal facilities at Children's National Medical Center and at the University of Maryland School of Medicine. The $D_5R^{-/-}$ knock-out mice and their ($D_5R^{+/+}$) wild-type littermates were identified by DNA genotyping. The studies were conducted in accordance with NIH guidelines for the ethical treatment and handling of animals in research and approved by the Children's National Medical Center Institutional Animal Care and Use Committee.

Co-Immunoprecipitation—Cell lysates from hPTCs were prepared using radioimmune precipitation assay lysis buffer (50 mM Tris-HCl, pH 7.4, 150 mM NaCl, 1% Triton X-100, 1% sodium deoxycholate, 0.1% SDS) supplemented with protease inhibitors (1 mM PMSF, 5 μg/ml aprotinin, and 5 μg/ml leupeptin). Equal amounts of cell lysates (300 μg protein) were mixed with 2 μg each of the immunoprecipitating Ab and incubated on a rocking platform at 4 °C overnight. Protein A/G plus beads were added to each sample and incubated further for 2 h at room temperature on a rocking platform. The bound proteins were eluted by the addition of Laemmli buffer. The samples were immunoblotted and visualized for proteins of interest via chemiluminescence (SuperSignal West Dura Substrate, Pierce) and autoradiography. The immunoprecipitates were run alongside with total cell lysates as positive control.

Förster Resonance Energy Transfer (FRET) Microscopy—FRET microscopy was performed as described previously (31, 32). HEK293-hD_5R cells were grown on coverslips and immunostained for hD_5R or SNX1 or both. V5-tagged D_5R was labeled with monoclonal anti-V5 Ab conjugated with Alexa Fluor 488 (Santa Cruz Biotechnology), which served as the donor fluorophore of the FRET dipole. The acceptor fluorophore was Alexa Fluor 555-conjugated to polyclonal anti-SNX1 Ab (Santa Cruz Biotechnology). FRET between appropriately labeled D_5R and SNX1 was performed using a Bio-Rad Radiance 2100 microscope system with the same gain for PMT1 (488-nm laser, channel 1) and PMT2 (543-nm laser, channel 2) with a 60× NA 1.4 objective lens (W. M. Keck Center for Cellular Imaging, University of Virginia, Charlottesville, VA). Corrected pFRET images were obtained by removing both donor and acceptor spectral bleed-through from unprocessed uFRET images (31). The percentage of energy transfer (E%) was calculated based on the equation of $E\% = 100 \times \{1 - I_{DA}/[I_{DA} + \text{pFRET}((\psi_{DD}/\psi_{AA})(Q_D/Q_A))]\}$, where D is donor alone, DA is donor and acceptor double-labeling, ψDD and ψAA are collection efficiencies in the donor and acceptor channels, and Q_D and Q_A are the quantum yields of the donor and acceptor, respectively (31).

Colocalization of D_5R and SNX1—Co-localization was performed in both cultured hPTCs and human kidney sections. hPTCs were grown on poly-D-lysine-coated coverslips (BD Biosciences) in 24-well plates and treated with fenoldopam (1 μM) for 15 min at the given time points. The cells were double-immunostained for SNX1 (BD Biosciences) and D_5R (Genetex), whereas the cell membrane was labeled with membrane-impermeant biotin and avidin-Cy5. To determine the effect of SNX1 depletion on D_5R trafficking, hPTCs were immunostained for D_5R, and the plasma membrane was labeled using wheat germ agglutinin conjugated with Alexa 555. Images were obtained sequentially in separate channels to avoid bleed-through using the Olympus IX-70 Laser Confocal Scanning Microscope with Plan Apo, 60×/1.4 NA oil immersion objective using 450-nm

excitation and 535-nm emission filters for Alexa 488- and 560-nm excitation and 645-nm emission filters for Alexa 568. Images were overlain using Olympus Fluoview FV300 version 3C Acquisition Software to determine colocalization.

Paraffin-embedded sections of normal human kidney (Imgenex) were double-immunostained as above after antigen retrieval using heat and pressure. Confocal and differential interference contrast images were obtained using Carl Zeiss LSM 510 META with 63×/1.4 NA oil immersion objective and processed using Zeiss 510 META with Physiology Software Version 3.5 and Multiple Time Series Software Version 3.5.

Silencing of SNX1 Expression—The expression of endogenous SNX1 in hPTCs was silenced via SNX1-specific siRNA (Qiagen) using Hiperfect transfection reagent (Qiagen). Non-silencing mock siRNA (Qiagen) and PBS (vehicle) were used as negative controls. The cells were grown for 48 h post-transfection before determination of cell surface receptors. The extent of SNX1 depletion was verified by immunoblotting.

Time-resolved Fluorometry—To quantify the D_5R surface membrane receptor density, time-resolved fluorometry was performed. hPTCs were grown in 96-well plates, and the endogenous SNX1 expression was silenced using SNX1-specific siRNA (Qiagen). The cells were treated with fenoldopam and then probed for surface D_5R under non-permeant conditions using rabbit anti-D_5R antibody (Genetex) that targets the third extracellular loop of the receptor and goat anti-rabbit IgG conjugated with europium (PerkinElmer Life Sciences). The europium bound to the remaining secondary antibodies was chemically released, and the europium fluorescence, which signifies the remaining receptors on the surface membrane, was quantified via time-resolved fluorometry using the VICTOR^3 V™ Multilabel Counter (PerkinElmer Life Sciences). The sample fluorescence was measured for 400 μs after a delay time of 400 μs using 340-nm excitation and 615-nm emission filters. DAPI fluorescence was used to normalize the results.

Determination of cAMP Production—hPTCs previously transfected with mock or SNX1-specific siRNA or vehicle as control and grown in 12-well plates were incubated in serum-free medium with the phosphodiesterase inhibitor 3-isobutyl-1-methylxanthine (1 μM; Calbiochem) for 3 h. The cells were then treated with fenoldopam (1 μM/30 min), dopamine hydrobromide (1 μM/30 min), or vehicle, washed 3 times with fresh medium, and re-challenged with fenoldopam or dopamine hydrobromide for another 30 min. The cells were washed copiously with PBS, and the intracellular cAMP levels were determined using the DetectX Direct cAMP assay (Arbor Assays) and the protein concentrations using a BCA Protein Assay kit (Pierce). The cAMP results were normalized for protein concentration.

Time-resolved, Non-radioactive GTP-europium (GTP-Eu) Binding Assay—We evaluated the binding of GTP-Eu (PerkinElmer Life Sciences) to D_5R-enriched plasma membranes in HEK293-hD_5R previously transfected with non-silencing mock or SNX5-specific siRNA and treated with fenoldopam (1 μM/15 min) or vehicle. The GTP-Eu binding assay was performed in Acro-Well filter plates under optimized conditions for D_5R. Briefly, 10 μg of membrane protein/sample was added to the assay solution (50 mM HEPES, 100 μg/ml saponin, 2 mM GDP, 125 mM NaCl, and 3 mM $MgCl_2$, pH 7.4). After a 30-min preincubation period with fenoldopam (2 μM) or vehicle, 10 nM GTP-Eu was added and incubated further for 30 min. The reaction was terminated by vacuum filtration followed by washing with wash buffer. The bound GTP-Eu was measured using Victor^3 V Multilabel Counter (340-nm excitation/615-nm emission, 0.4-ms delay, 0.4-ms window).

Cellular Sodium Transport Studies—SNX1-depleted hPTCs were grown to confluence under polarized conditions on Corning HTS Transwell supports inserted in 12-well plates and incubated at 37 °C incubator with humidified 5% CO_2 in 95% air. The cells were serum-starved for 2 h and treated with fenoldopam (1 μM, 15 min) or vehicle (PBS, as control) at the basolateral area. After washing, the cells were incubated with the permeant sodium indicator sodium green tetraacetate (5 μM, Molecular Probes) in complete medium without phenol red. The cells were washed with PBS, and the fluorescence signal for each Transwell was measured using the VICTOR^3 V™ Multilabel Counter (excitation 485 nm and emission 535 nm). Ouabain (50 μM, 1 h) was used to inhibit Na^+,K^+-ATPase activity.

Expression Profiling of Select Genes—Total cell lysates and plasma membrane-enriched fractions were prepared from hPTCs transfected with SNX1-specific siRNA or non-silencing mock siRNA or vehicle as controls. Uniform amounts of protein were resolved via 10% SDS-PAGE and electro-transferred onto nitrocellulose membrane, and the membrane was blocked using 5% dry nonfat milk. Thereafter, the membrane was probed for D_5R (Genetex), D_1R (Origene) or angiotensin II type 1 receptor (AT_1R; Santa Cruz Biotechnology). Renal cortical lysates from D_5R knock-out mice and wild-type littermates were also prepared and probed for endogenous Snx1 (ProteinTech).

siRNA-mediated Renal Cortical Silencing of Snx1 and Renal Clearance Studies—Uninephrectomized adult male C57BL/6J and BALB/cJ mice were anesthetized with pentobarbital (50 mg/kg body weight) intraperitoneally, tracheotomized, and placed on a heated board to maintain rectal temperature at 37 °C. A polyethylene delivery tube connected to a mini-osmotic pump (ALZET® Osmotic Pump) was inserted and positioned subcapsularly to continuously deliver the Snx1-specific siRNA at a rate of 12 μl/day for 7 days. The siRNA was prepared in an *in vivo* transfection reagent (Mirus Bio) under sterile conditions. The tube was kept in place using a drop of surgical glue on top of the renal capsule, whereas the pump was secured onto the abdominal wall by a suture to prevent dislodgement. Infusion of vehicle or non-silencing mock siRNA (Qiagen) served as controls. The systolic and diastolic blood pressure were measured (Cardiomax II) from the aorta via the femoral artery (12, 33) before and after the 7-day siRNA infusion. At the end of the study, the siRNA-transfected kidney was removed before the mice were euthanized via a lethal dose of CO_2 by inhalation followed by decapitation to confirm death while still under anesthesia.

A separate set of uninephrectomized BALB/cJ mice renally infused for 7 days with non-silencing mock or Snx1-specific siRNA were anesthetized with pentobarbital (50 mg/kg body weight, intraperitoneal) before cannulation of the femoral artery (for blood pressure monitoring), femoral vein (for the

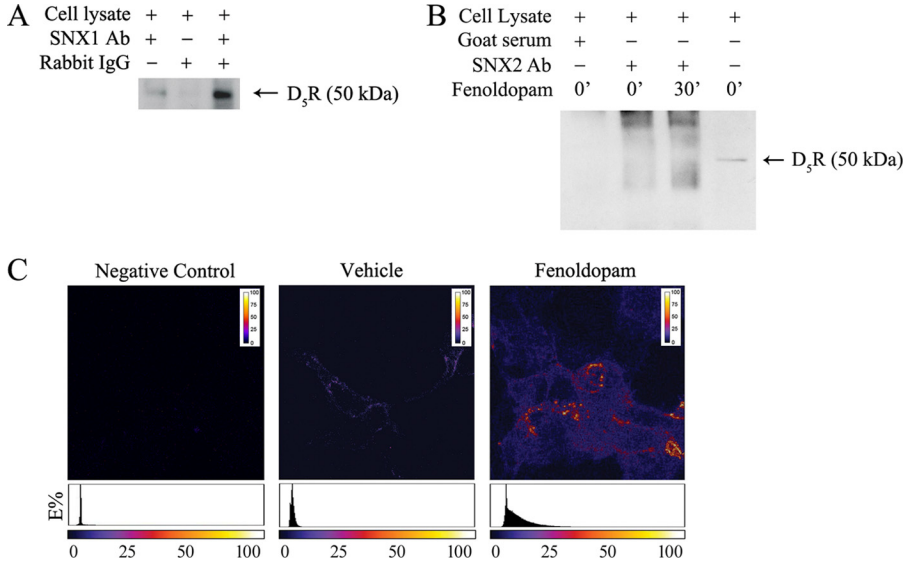

FIGURE 1. **Interaction between D_5R and SNX1.** *A*, precleared cell lysates from hPTCs were immunoprecipitated with monoclonal anti-SNX1 Ab or normal mouse IgG (negative control) and immunoblotted for human D_5R (~50 kDa). Total cell lysate was used as a positive control. *B*, precleared lysates from hPTCs treated with the D1-like receptor agonist fenoldopam (1 μM, indicated time points) were immunoprecipitated with goat polyclonal anti-SNX2 Ab or normal goat serum (negative control) and immunoblotted for human D_5R (~55 kDa). Total cell lysate was used as the positive control. *C*, HEK293 cells heterologously expressing V5-tagged human D_5R treated with vehicle or fenoldopam (1 μM, 15 min) were prepared for FRET microscopy. V5-tagged D_5R was labeled with monoclonal anti-V5 primary Ab conjugated with Alexa488 (the donor fluorophore of the dipole), whereas SNX1 was labeled with polyclonal anti-SNX1 Ab conjugated with Alexa555 (the acceptor fluorophore). The corrected pFRET (*upper panel*) and corresponding energy transfer efficiency (*E*%, *lower panel*) are shown. Negligible FRET signal was observed when the primary antibodies were omitted (negative control).

infusion of fenoldopam), and jugular vein (for sodium loading and fluid maintenance). A PE-90 catheter was also inserted through a cystotomy and secured onto the bladder wall for urine collection. A normal saline load equivalent to 5% of body weight was infused intravenously for 30 min. Thereafter, urine samples were collected every hour starting with baseline followed by the treatment period (fenoldopam, 2 μg/kg/min intravenously for 1 h) and then a recovery period. Urine Na^+ was analyzed using Synchron EL-ISE Electrolyte system (Beckman). UNaV was calculated as urine volume × Na^+ (mEq/liter).

Statistical Analysis—When applicable, data are expressed as the means ± S.E. Significant difference between two groups was determined by Student's *t* test, whereas that among groups was determined by one-way ANOVA followed by Holm-Sidak or Fisher post-hoc test. $p < 0.05$ was considered significant. Statistical analysis was performed using SigmaStat 3.5 (SPSS).

RESULTS

D_5R interacts with SNX1—We initially confirmed the physical interaction between the D_5R and SNX1 (18) through co-immunoprecipitation using cell lysates of immortalized hPTCs. In these cells the endogenous D_5R was pulled down by an anti-SNX1 Ab (Fig. 1*A*). Because SNX1 and SNX2 have been demonstrated to have functional redundancy (34), we also evaluated the interaction between D_5R and SNX2 in hPTCs and found that these two proteins did not co-immunoprecipitate even after agonist stimulation (Fig. 1*B*).

We next evaluated the dynamics of the D_5R-SNX1 interaction via FRET microscopy of HEK293 cells expressing V5-tagged D_5R (HEK293-hD_5R). The FRET signal becomes apparent when the proteins of interest tagged with the appropriate donor and acceptor fluorophores are within 10 nm of each other and is reported as the efficiency of energy transfer (*E*%). The cells were evaluated at basal condition and after treatment with the D_1-like receptor agonist fenoldopam. There is no agonist that can discriminate between D_1R and the D_5R, but because HEK293 cells do not endogenously express either receptor, fenoldopam exerted its effect only on the heterologously expressed D_5R. In vehicle-treated controls, the interaction between D_5R and SNX1 was observed primarily at the membrane rather than at the cytoplasm (membrane, *E*% = 21.6 ± 3.2% *versus* cytoplasm *E*% = 4.4 ± 1.6%) (Fig. 1*C*). Treatment with fenoldopam (1 μM) markedly enhanced the interaction between the two proteins and promoted their internalization (membrane, *E*% = 17.3 ± 3.4% *versus* cytoplasm, *E*% = 34.8 ± 4.6%). Negligible FRET signal was observed in the absence of the primary Ab (negative control).

We also determined the extent and localization of the D_5R-SNX1 interaction in hPTCs through laser scanning confocal microscopy. Endogenous D_5R was basally distributed at the cell membrane and cytoplasm, whereas endogenous SNX1 was found to a greater extent in the cytoplasm than at the cell membrane (Fig. 2*A*). Colocalization was evident mostly at the cell membrane. Fenoldopam (1 μM) treatment for 5 min resulted in D_5R internalization and increased colocalization with SNX1 at the cytoplasm and then at the perinuclear area after 15 min of agonist treatment. Both D_5R and SNX1 redistributed to the cytoplasm and membrane after 30 min of agonist treatment, suggesting recycling of the receptors and their subsequent reinsertion to the plasma membrane.

The colocalization of the D_5R and SNX1 was not restricted to cells *in vitro* but was also demonstrated in human kidney sections. The D_5R was abundantly expressed in the brush border and cytoplasm of renal proximal tubules and, to a lesser degree, in the glomeruli. SNX1 was expressed in renal proximal tubules

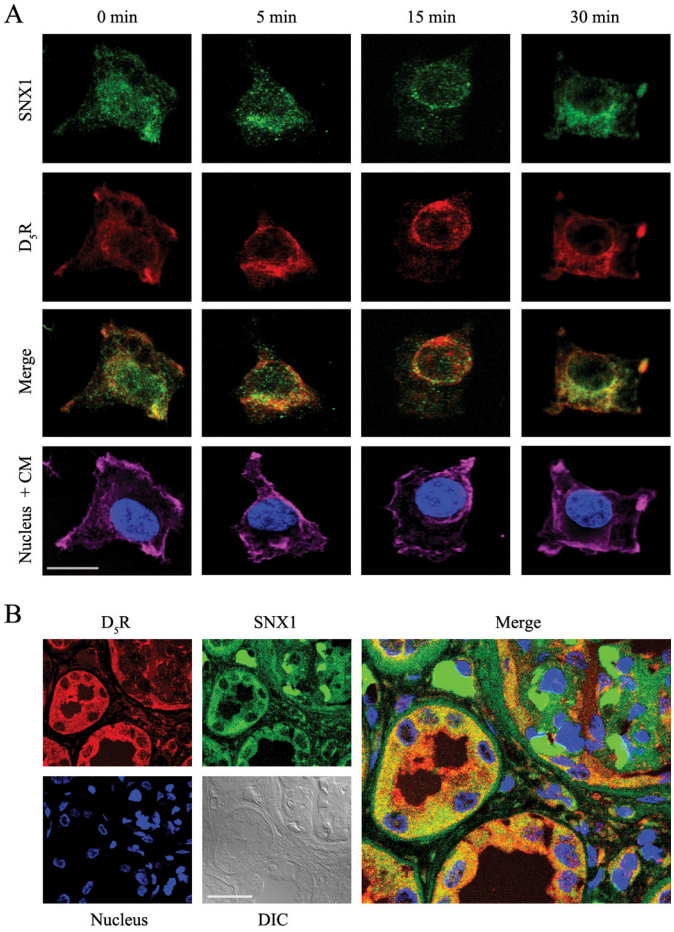

FIGURE 2. **Colocalization of D_5R and SNX1 in human proximal tubule cells and human kidney.** *A*, hPTCs were grown on coverslips, serum-starved for 1 h, and treated with fenoldopam (1 μM) at the indicated time points. The cells were then fixed, permeabilized, and double-immunostained for endogenous SNX1 (pseudocolored *green*) and D_5R (pseudocolored *red*). Punctate areas of colocalization are in *yellow*. A membrane-impermeant biotin was used to label the cell membrane (*CM*), whereas DAPI was used to label the nucleus. *B*, paraffin-embedded sections of normal human kidney were double immunostained for endogenous D_5R (pseudocolored *red*) and SNX1 (pseudocolored *green*) after antigen retrieval using heat and pressure. DAPI was used as nuclear stain. The images were obtained by laser scanning confocal microscopy at 600× magnification. *Bars* = 20 μm. *DIC*, differential interference contrast.

and the glomeruli. Both colocalized strongly in the renal proximal tubules (Fig. 2*B*).

SNX1 Is Required for D_5R Internalization—To determine the role of SNX1 on D_5R trafficking in hPTCs, we silenced the expression of endogenous SNX1 via siRNA (Fig. 3*A*) and evaluated the translocation of the receptors upon agonist stimulation via confocal microscopy (Fig. 3*B*). To delineate plasma membrane-bound *versus* cytoplasmic receptors, the plasma membrane was labeled using wheat germ agglutinin (pseudocolored red), whereas the receptors were immunostained using a specific rabbit anti-SNX1 Ab (pseudocolored green). In control cells, the D_5R was observed to be localized to both the plasma membrane and cytoplasm. Agonist stimulation resulted in receptor endocytosis after 5 and 15 min of fenoldopam treatment. Colocalization of D_5R and the plasma membrane was again observed after 30 min of agonist stimulation, which may signify receptor recycling. In SNX1-depleted cells, D_5R was distributed in both the plasma membrane and the cytoplasm in a manner similar to that observed in control cells; however, there was failure of D_5R to internalize after agonist activation. These results indicate that SNX1 is required for D_5R endocytosis upon agonist stimulation but not for basal receptor trafficking.

We confirmed the role of SNX1 on D_5R trafficking by measuring the surface receptor density in SNX1-depleted cells via time-resolved europium fluorometry. We treated the cells with the D_1-like receptor agonist fenoldopam for 15 min and then with vehicle (PBS) after copious washing to allow the receptors to recycle back to the plasma membrane. About 46 ± 3 and 41 ± 2% of surface D_5R internalized after fenoldopam (1 μM) treatment in both untransfected control and non-silencing mock siRNA-transfected cells, respectively (Fig. 3*C*). Withdrawal of fenoldopam resulted in the recycling of the receptors back to the plasma membrane (78 ± 1 and 77 ± 2%, 84 ± 4 and 90 ± 2%, and 100 ± 1 and 104 ± 2% at 15, 30, and 60 min after fenoldopam treatment in untransfected and mock siRNA-transfected cells, respectively). However, no appreciable change in the surface receptor density was observed in SNX1-depleted cells.

Loss of SNX1 Activity Abrogates D_5R-mediated cAMP Production, GTP Binding, and Sodium Transport Inhibition—We first assessed the functional correlate of SNX1 depletion by determining the cAMP response to agonist activation of D_5R. Treatment with the D_1-like dopamine receptor agonist fenoldopam resulted in increased cAMP levels in control cells transfected with vehicle (181.6 ± 17.7%) or non-silencing "mock" siRNA (194.7 ± 7.6%) (Fig. 4*A*). A second challenge with the agonist resulted in the blunting of the cAMP response in cells transfected with vehicle (95.5 ± 7.0%) or non-silencing mock siRNA (92.8 ± 3.7%), indicating receptor desensitization. In contrast, there was no change in cAMP levels after fenoldopam stimulation in SNX1-depleted cells. SNX1 silencing did not modify the basal cAMP levels.

To demonstrate the physiological relevance of SNX1 in D_5R signaling, we also used the natural ligand for all the dopamine receptors, *i.e.*, dopamine. Treatment with dopamine resulted in increased cAMP production in cells treated with vehicle (133.8 ± 8.4%) and mock siRNA (129.2 ± 11.9%) compared with basal levels, whereas successive treatment with dopamine attenuated the cAMP production in both cells (95.5 ± 13.7 and 86.2 ± 10.6%, respectively) (Fig. 4*B*). In contrast, dopamine treatment in SNX1-depleted cells resulted in a decrease in cAMP production (70.6 ± 3.9%) that further decreased after another challenge with dopamine.

To explain the observed cAMP response to fenoldopam and dopamine, we next determined the extent of binding of non-hydrolyzable GTP-Eu to D_5R-enriched plasma membranes. This assay reflects the binding of GTP-Eu to $G\alpha_s$ in exchange for GDP, resulting in the activation of the $G\alpha_s$ for downstream signaling. We used the plasma membranes from SNX1-depleted HEK293-hD_5R and control cells that were previously stimulated with fenoldopam or vehicle. Although HEK293 cells endogenously express trace amounts of either D_1R or D_5R,[4] these cells fail to increase cAMP production in response to ago-

[4] V. A. M. Villar, J. E. Jones, I. Armando, L. D. Asico, C. S. Escano, Jr., H. Lee, X. Wang, Y. Yang, A. M. Pascua-Crusan, C. P. Palmes-Saloma, R. A. Felder, and P. A. Jose, unpublished information.

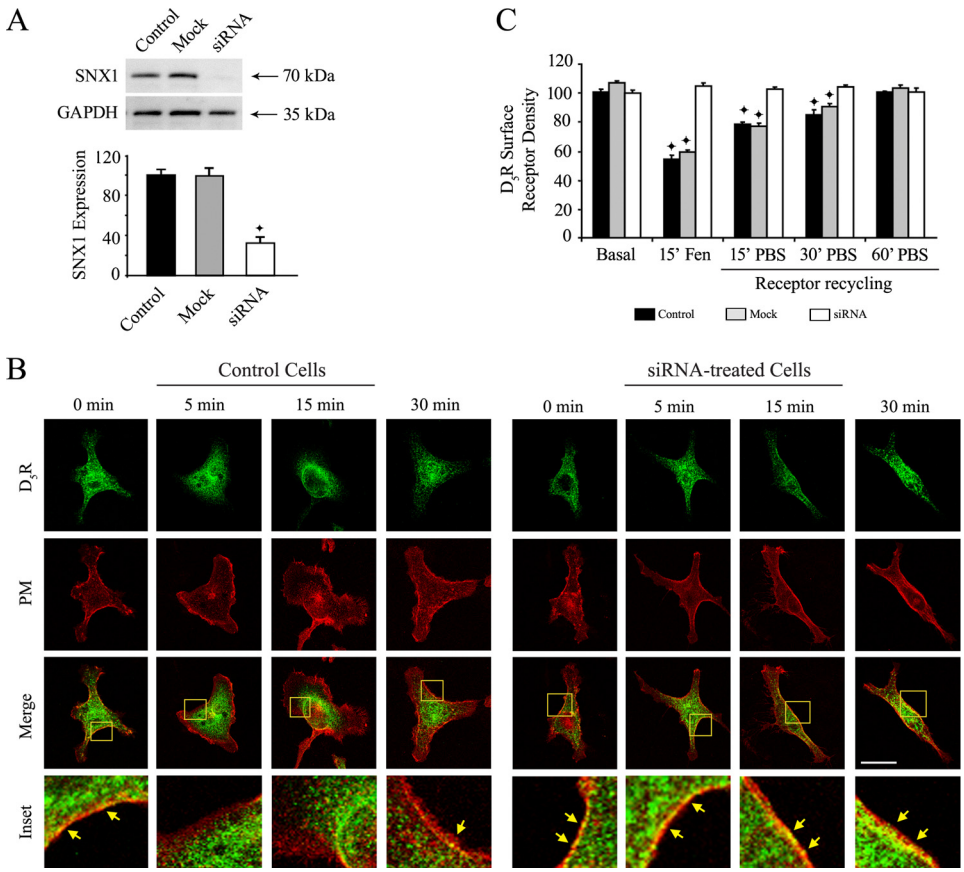

FIGURE 3. **Effect of SNX1 depletion on D_5R endocytosis in human renal proximal tubule cells.** *A*, total cell lysates were prepared from hPTCs previously transfected with SNX1-specific siRNA (*siRNA*), non-silencing siRNA (*Mock*), or vehicle (*Control*) and immunoblotted for SNX1. Values are expressed as the mean ± S.E. ◆, $p < 0.05$, *versus* others, one-way ANOVA and Holm-Sidak post-hoc test, $n = 3$/group. *B*, the expression of endogenous SNX1 was silenced using SNX1-specific siRNA, and D_5R trafficking was evaluated using confocal microscopy. D_5R endocytosis was induced using fenoldopam (1 μM) at the given time points. The plasma membrane was visualized using wheat germ agglutinin-Alexa 555 (pseudocolored *red*) and D_5R using polyclonal rabbit anti-D_5R Ab and donkey anti-rabbit Ab-Alexa 488 (pseudocolored *green*). The localization of the receptor in the plasma membrane is indicated by *yellow punctate* areas in *merge* and *inset* images (with *yellow arrows*). The images were obtained by laser scanning confocal microscopy at 600× magnification. *Bars* = 20 μm *C*, the expression of endogenous SNX1 was silenced using SNX1-specific siRNA, and the surface receptor density was quantified via time-resolved europium fluorometry. The cells were probed with rabbit polyclonal anti-D_5R Ab (which targets the third extracellular loop of the receptor) and re-probed with goat anti-rabbit Ab conjugated with europium. An enhancer solution was used to chemically release the europium, giving off a very strong fluorescent signal upon release. The signal, indicating the D_5R density, was quantified using a VICTOR^3 V™ Multilabel Counter. DAPI was used for normalization. ◆, $p < 0.05$, *versus* Basal (one-way ANOVA, followed by Holm-Sidak post-hoc test; $n = 3$, performed in duplicates). *Fen*, fenoldopam.

nists (35), hence the observed response in these cells were those of the heterologously expressed D_5R. Stimulation with fenoldopam resulted in increased GTP-Eu binding in both untreated and treated membranes (146 ± 33 and 158 ± 76 absorbance units, respectively) of mock siRNA-treated control cells, indicating the presence of functional D_5R-associated G proteins (Fig. 4*C*). However, there was negligible GTP-Eu binding in the membranes from SNX1-depleted cells in response to agonist stimulation, suggesting that SNX1 may be important in the activation of D_5R-associated $G\alpha_s$.

In another set of experiments, we determined the effect of SNX1 depletion on D_5R-mediated sodium transport in hPTCs loaded with the fluorescent dye sodium green by monitoring the change of the fluorescence emission after fenoldopam treatment at the basolateral side to target the Na^+,K^+-ATPase (Fig. 4*D*). In control cells, D_5R stimulation resulted in increased intracellular sodium (10 ± 1%), indicating the ability of activated D_5R to inhibit sodium transport across the basolateral membrane. In SNX1-depleted cells, fenoldopam treatment resulted in decreased intracellular sodium (−9 ± 2%), indicating the failure of D_5R to inhibit Na^+,K^+-ATPase, which normally pumps Na^+ extracellularly in exchange for K^+. Fenoldopam had no effect when cells were pretreated with ouabain (50 μM, 1 h) at the basolateral side (data not shown), indicating that the D_5R effect was exerted on Na^+,K^+-ATPase.

SNX1 Knockdown Increases AT_1R Expression—Previous studies from our laboratory have shown that D_5R negatively regulates the expression of AT_1R in renal proximal tubule cells (14, 32). To determine whether the SNX1-mediated D_5R dysfunction results in the failure of the D_5R to keep AT_1R expression in check, SNX1 expression was silenced in hPTCs via siRNA. In SNX1-depleted cells, both native (~45 kDa) and glycosylated (~70 kDa) forms of total AT_1R (32) were increased by 28 ± 4 and 29 ± 3%, respectively, compared with control cells (Fig. 4*E*). Transfection with mock siRNA did not alter the AT_1R expression. The increase in AT_1R expression is not due to a direct interaction with SNX1 as these two proteins do not co-immunoprecipitate in proximal tubule cells from normotensive WKY rat and SHR or in HEK293 cells (Fig. 4*F*). We also evaluated the distribution of AT_1R in plasma membrane-enriched

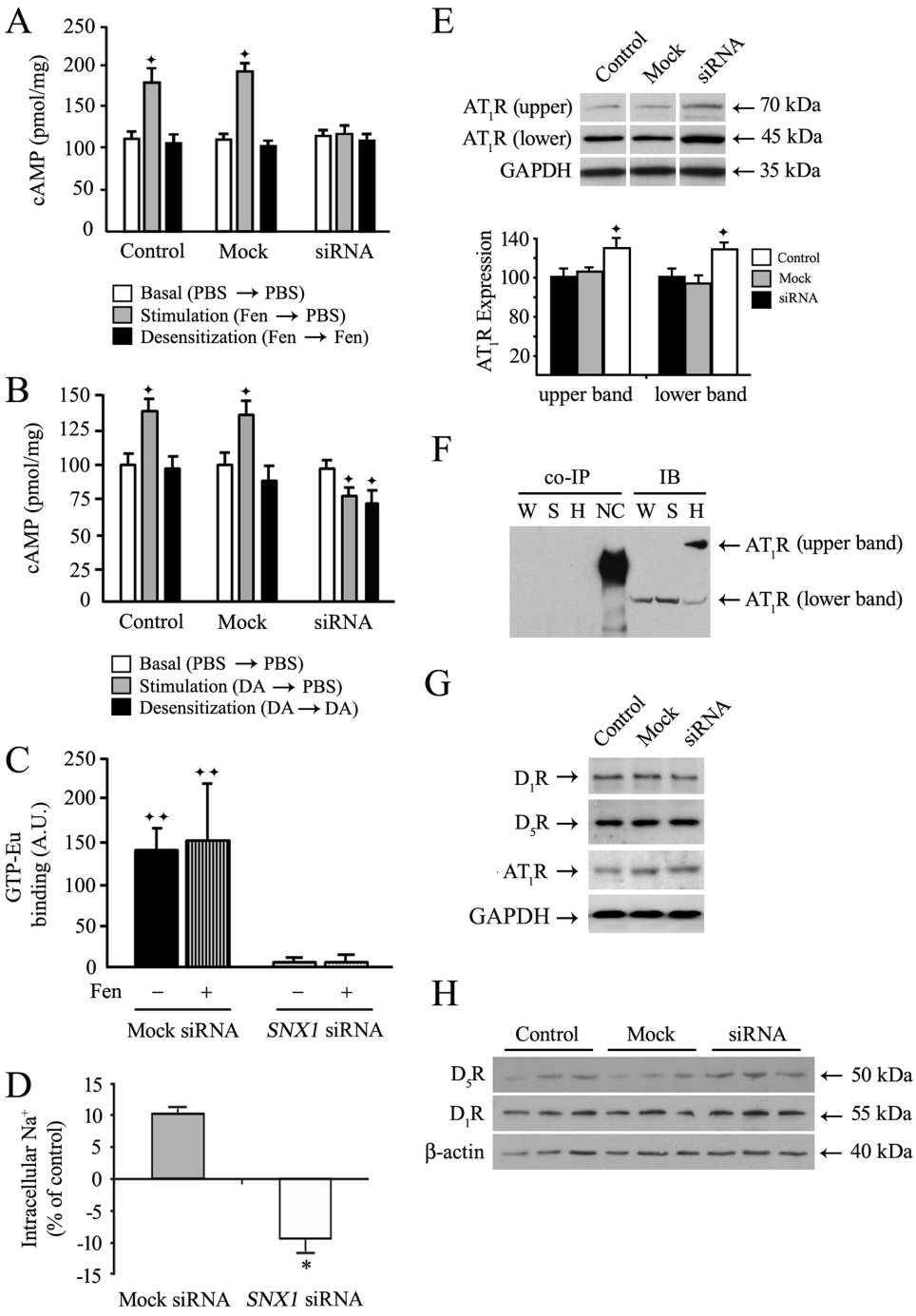

FIGURE 4. **Effects on cAMP production, sodium transport, and expression profiles of AT_1R and SNX1.** *A* and *B*, cAMP levels in hPTCs were pretreated with the phosphodiesterase inhibitor 3-isobutyl-1-methylxanthine and stimulated with fenoldopam (*Fen*; 1 μM, 30 min) (*A*) or dopamine (*DA*; 1 μM/30 min) (*B*), washed, and re-challenged with fenoldopam (1 μM, 30 min) or dopamine (1 μM/30 min). cAMP levels were normalized for total protein. *C*, shown is binding of GTP-Eu to D_5R-enriched membranes of HEK293-hD_5R cells previously transfected with either non-silencing mock or *SNX1*-specific siRNA and treated with fenoldopam (1 μM, 30 min) or vehicle. GTP-Eu intensities (absorbance units (*A.U.*)) indicate the bound and retained GTP-Eu in the membrane. *D*, shown is the change in intracellular sodium *green* in hPTCs that were transfected with non-silencing (*Mock siRNA*) or *SNX1*-specific siRNA (*SNX1 siRNA*) and treated with fenoldopam (1 μM, 15 min) or vehicle. *E*, shown are expression profiles of the glycosylated (*upper*) and non-glycosylated forms of AT_1R in hPTCs that were transfected with *SNX1*-specific silencing siRNA (*siRNA*), non-silencing mock siRNA (*Mock*), or vehicle (*Control*). GAPDH was used for normalization. Values are expressed as the mean ± S.E. ◆, $p < 0.05$, *versus* others, one-way ANOVA followed by Holm-Sidak post hoc test, $n = 3$–4/group in duplicates (for *A*, *B*, and *E*) ◆◆, $p < 0.05$, *versus SNX1* siRNA, one-way ANOVA followed by Fisher post hoc test, $n = 4$/group in triplicates (for C). *, $p < 0.05$, *versus* control, Student's *t* test, $n = 3$/group in duplicates. *F*, total cell lysates from WKY (*W*) and SHR (*S*) renal proximal tubule cells and HEK293 (*H*) cells were immunoprecipitated with a mouse monoclonal anti-SNX1 Ab or normal mouse IgG (negative control (*NC*)) and immunoblotted (*IB*) for AT_1R (co-immunoprecipitated (*co-IP*)). Regular immunoblotting of total cell lysates were used as positive control. *G*, plasma membrane-enriched fractions were prepared from SNX1-depleted hPTCs and immunoblotted for proteins of interest. Non-silencing (*Mock*) siRNA or vehicle (*Control*) was used as the negative control. $n = 3$/group. *H*, hPTCs were transfected with SNX1-specific siRNA or non-silencing mock siRNA (*Mock*) or vehicle (*Control*) for 48 h. Total cell lysates were prepared and immunoblotted for D_5R, D_1R, and β-actin as reference.

fractions of hPTCs and found that there was no difference in the abundance of AT_1R in SNX1-depleted cells compared with control cells (Fig. 4*G*).

The expression of D_5R was unchanged after SNX1 depletion (Fig. 4*H*). Because the D_1-like receptors interact with and regulate each other (3), we determined if SNX1 depletion alters the basal D_1R expression and found that D_1R expression in SNX1-depleted cells was similar to that of control cells (Fig. 4*H*). The abundance of both D_1-like dopamine receptors in the plasma membrane of SNX1-depleted cells was also similar to that of control cells (Fig. 4*G*).

Renal Snx1 Depletion Increases AT_1R Expression in Mice—To determine if the loss of SNX1 translates into discernable phenotypes, we infused *Snx1* siRNA into the left kidney of uninephrectomized C57BL/6J and BALB/cJ mice via minipump for 7 days to selectively down-regulate renal SNX1 expression. Infusion of *Snx1* siRNA in C57BL/6J and BALB/cJ mice resulted in a 50% reduction of renal SNX1 expression (Fig. 5*A*). In agreement with the *in vitro* data, renal loss of SNX1 resulted in a 133 ± 7 and 140 ± 4% increase of non-glycosylated and glycosylated forms of AT_1R, respectively, compared with control groups (Fig. 5*B*). However, there was no appreciable difference in either renal D_5R or D_1R expression with SNX1 depletion (Fig. 5*C*). Similarly, SNX1 depletion in BALB/cJ mice resulted in a 216 ± 10 and 144 ± 4% increase in the non-glycosylated and glycosylated forms of AT_1R, respectively, compared with controls (Fig. 5*B*). The SNX1 expression in the liver and heart was unchanged after renal SNX1 depletion (Fig. 5*D*). There was also no difference in SNX1 expression in $D_5R^{-/-}$ mice compared with wild-type littermates (Fig. 5*E*).

Renal SNX1 Depletion Results in Elevated Blood Pressure and Blunted Natriuretic Response to Fenoldopam in Mice—SNX1 depletion results in the loss of D_5R function, which in turn increases AT_1R abundance, changes that are pro-hypertensinogenic. Thus, we measured the blood pressure in mice before and after the renal subcapsular infusion of *Snx1* siRNA or vehicle. We found that both the systolic and diastolic blood pressures (under pentobarbital anesthesia) were higher by 13 and 15 mm Hg in SNX1-depleted C57BL/6J mice and by 26 and 23 mm Hg in SNX1-depleted BALB/cJ mice compared with controls (Fig. 5*F*), indicating that SNX1 may play a crucial role in blood pressure regulation through its effect on D_5R function and in turn on AT_1R expression. Baseline systolic and diastolic blood pressures were not different before siRNA infusion. There was also no change in the heart rates among the groups before or after the siRNA infusion (data not shown).

We next tested the ability of renal SNX1-depleted BALB/cJ mice to respond to fenoldopam in terms of renal sodium excretion. Fenoldopam treatment resulted in a 40.5 ± 24.1% increase in urinary Na^+ excretion (UNaV) compared with basal levels in mock siRNA-infused mice (Fig. 5*G*), demonstrating a normal natriuretic response to fenoldopam stimulation in control mice and a compensatory decrease in UNaV during the recovery period. However, there was no natriuretic response to fenoldopam stimulation in renal SNX1-deficient mice (−13.8 ± 13.4% change from basal), indicating the impairment of the D_1-like dopamine receptors with SNX1 depletion. The further decrease in the UNaV during the recovery period may conceivably be due to the anti-natriuretic effect of AT_1R, which was increased basally in SNX1-deficient mice (Fig. 5*B*), or to the preponderance of the activity of the D_2-like dopamine receptors in response to endogenously produced dopamine; the renal proximal tubules produce dopamine from filtered L-DOPA.

Blood pressure was also measured hourly before (basal), during (treatment), and after (recovery) fenoldopam infusion. Both systolic and diastolic blood pressures were consistently higher in SNX1-deficient mice compared with controls (Fig. 5, *H* and *I*). However, there was no difference in blood pressure during all three periods for each group of mice. The fenoldopam was infused at a dose that promotes natriuresis but does not affect the blood pressure (36). A higher dose of fenoldopam is required to affect systemic blood pressure; however, this dose would target other receptors, *e.g.,* serotonin receptor (37) and the D_2-like dopamine receptors, among others, which may confound the interpretation of the results.

DISCUSSION

The trafficking of D_5R is not well understood. We now show for the first time the spatial and temporal aspects of agonist-activated D_5R trafficking and underscore the important role of SNX1 in this process in hPTCs. Heydorn *et al.* (18) previously reported that SNX1 interacted with the carboxyl terminus of D_5R. We confirmed this interaction and further elucidated the distribution of the D_5R and SNX1 in hPTCs and the human kidney. In hPTCs, D_5R is found at the plasma membrane and cytoplasm in the basal state, in contrast to the predominantly intracellular expression of D_1R (38), although D_1R is localized to the plasma membrane in neuroblastoma cells NG108–15 (39). On the other hand, SNX1 exists in both membrane and cytoplasmic pools in hPTCs, similar to previous observations in HeLa cells. Both D_5R and SNX1 are abundantly expressed and colocalize in proximal tubules of the human kidney.

The dynamics of D_5R-SNX1 interaction in HEK293 cells expressing the human D_5R were evaluated using FRET microscopy, which is an effective molecular indicator of physical coupling (31). The weak FRET signal observed basally may indicate basal receptor trafficking, in agreement with a previous report that the D_5R is constitutively active (40). Fenoldopam treatment increases the association of D_5R with SNX1 at the cytoplasm, indicating agonist-directed receptor endocytosis. These observations agree with those made in colocalization studies in hPTCs.

Previous reports showed that SNX1 residing in endosomes directs and promotes the endosome-to-lysosome degradative sorting of EGF receptor (22) and PAR1 (protease-activated receptor 1) (25) and the retrieval of the mannose 6-phosphate receptor from early endosomes to the trans-Golgi network (41) and directs the activated $P2Y_1$ to recycle via the slow recycling pathway (27). Interestingly, our studies demonstrate that SNX1 functions at a much more proximate step in D_5R trafficking, *i.e.,* internalization of the activated receptor. Initial GPCR sorting has been shown to occur at the plasma membrane through receptor modification to determine the fate of the receptor during subsequent intracellular trafficking and through lateral segregation of receptors across the surface membrane (42). The role of SNX1 in GPCR trafficking may be distinct from its con-

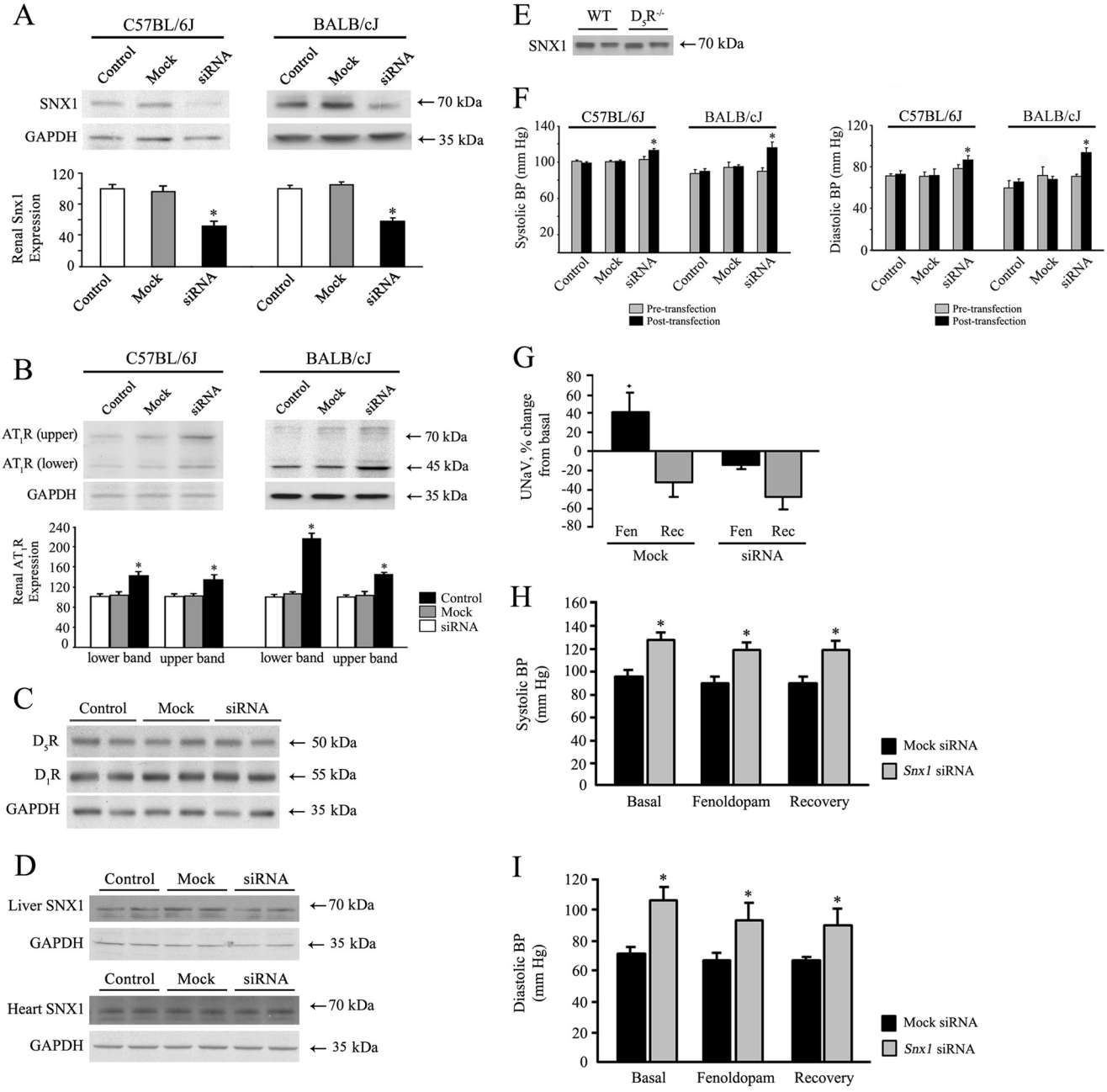

FIGURE 5. **Effect of renal Snx1 depletion on AT_1R expression and blood pressure in C57BL/6J and BALB/cJ mice.** The left kidney of age-matched, uninephrectomized adult mice were continuously infused with Snx1-specific siRNA via minipump for 7 days. Non-silencing, mock siRNA (*Mock*) or vehicle (*Control*) served as controls. *A–D*, the kidney, liver, and heart were harvested, and total homogenates were prepared for immunoblotting. The kidney homogenates were immunoblotted for SNX1 (*A*), AT_1R (*B*), and D_1R and D_5R (*C*). The liver and heart homogenates were also immunoblotted for SNX1 (*D*). GAPDH was used as the housekeeping protein. Representative images are shown. Values are expressed as the mean ± S.E. *, $p < 0.05$, *versus* others, one-way ANOVA followed by Holm-Sidak post-hoc test, $n = 3–4$/group. *E*, renal cortices from $D_5R^{-/-}$ mice and wild-type (*WT*) littermates were prepared and immunoblotted for endogenous SNX1. *F*, the systolic and diastolic blood pressures were measured via the femoral artery under pentobarbital anesthesia before and after a 7-day siRNA infusion. Data are expressed as the mean ± S.E. *, $p < 0.05$, *versus* others, one-way ANOVA followed by Holm-Sidak post-hoc test; $n = 3–4$/group. *G*, shown is percentage change of UNaV (calculated as urine volume × Na^+ (mEq/liter) from basal during a 1-h fenoldopam (*Fen*) infusion and the succeeding 1-h recovery (*Rec*) period. ◆, $p < 0.05$, *versus* others, one-way ANOVA followed by Fisher post-hoc test; $n = 4–5$/group. *H* and *I*, shown are systolic and diastolic blood pressures (*BP*) measured under pentobarbital anesthesia (50 mg/kg body weight, intraperitoneal) of uninephrectomized, salt-loaded, renal SNX1-deficient BALB/cJ before (*Basal*), during (*Fenoldopam*), and after (*Recovery*) infusion of fenoldopam (2 μg/kg/min for 1 h). *, $p < 0.5$, *versus* mock siRNA, one-way ANOVA, Holm-Sidak post-hoc test, $n = 3–5$/group.

served role in endosome-to-*trans*-Golgi network trafficking of cargo receptors. It is conceivable that SNX1 initiates the sorting of activated D_5R at the plasma membrane by tagging the receptor to a specific post-endocytic route where SNX1 plays a role. Alternatively, it is possible that SNX1, behaving as a peripheral membrane protein (17), may act as a scaffold or adaptor protein to facilitate the organization of D_5R and other membrane-bound or intracellular signaling components in phosphoinositide-enriched membrane microdomains (42, 43).

The functional relevance of the D_5R/SNX1 interaction is demonstrated by the failure of agonist-stimulated D_5R to elicit a cAMP response in hPTCs depleted of their endogenous SNX1

pool. The silencing of SNX1 expression completely blunts the ability of fenoldopam to increase intracellular cAMP levels, although fenoldopam stimulates both D_1-like receptors (D_1R and D_5R). There is no pharmacological agent available that could discriminate between the two receptors. D_1R does not interact with SNX1 (18). It is conceivable that both D_1-like dopamine receptors may heterodimerize with each other, and their ability to form dimers may be required for their activity in response to an agonist. The genetic ablation of D_5R alone (12) or any of the other dopamine receptors (44) results in elevated blood pressure, indicating that the loss of just one dopamine receptor subtype is sufficient to foster hypertension in mice. In contrast, stimulation with the natural ligand dopamine resulted in a decrease in cAMP production in SNX1-depleted hPTCs, suggesting the predominance of D_2-like dopamine receptor activity concomitant with D_5R impairment. The D_1-like dopamine receptors couple to stimulatory G proteins $G\alpha_s$ and $G\alpha_{olf}$ to stimulate adenylyl cyclase activity, resulting in increased cAMP production, whereas the D_2-like dopamine receptors normally couple to inhibitory G proteins $G\alpha_i$ and G_o leading to the inhibition of adenylyl cyclase activity and thus a decrease in cAMP production (8, 9).

The blunted cAMP response in SNX1-deficient HEK293-hD_5R cells may be explained by the inability of D_5R-enriched membranes to bind GTP-Eu in these cells, suggesting the failure of $G\alpha$ activation upon fenoldopam stimulation of D_5R. The negligible GTP-Eu binding in the absence of SNX1 suggests the requirement for SNX1 in either the association of D_5R with a G protein or the binding of the GTP to the $G\alpha$ subunit in these cells.

The failure of agonist-stimulated D_5R to internalize in the absence of SNX1 may also contribute to the lack of sustained cAMP production by the receptor. A new concept of "non-classical" GPCR signaling proposes that receptor internalization followed by trafficking through the phosphatase-containing endosomal compartments is involved in restoring receptor resensitization and responsiveness (45). We have reported that protein phosphatase 2A is important in the resensitization of the D_1R (46). G proteins and adenylyl cyclases are also present in endosomes where signaling from internalized receptors continues (45, 47, 48). We have reported that the internalized D_1R can increase cAMP production in response to a cell-permeable D_1-like receptor agonist (35). This persistent cAMP response can lead to both quantitative and qualitative differences in signaling outcomes (49). Thus, the failure of the agonist-stimulated D_5R to internalize precludes not just its ability to resensitize but also its continued ability to stimulate a cAMP response intracellularly.

The blunted cAMP response may also explain the failure to inhibit sodium transport upon fenoldopam treatment in SNX1-depleted cells. In the renal proximal tubule and medullary thick ascending limb of Henle (mTAL), D_1-like receptor stimulation inhibits sodium transporters such as Na^+/H^+ exchanger 3, $Na^+/HCO3^-$ co-transporter, $Cl^-/HCO3^-$ exchanger, and Na^+,K^+-ATPase (2, 3, 10) to promote sodium excretion. In humans with essential hypertension and in SHRs, there is a failure of the normal D_1-like receptor inhibition of these sodium transporters in the renal proximal tubule and mTAL (2, 3, 10). These observations underscore the need for an intact SNX1 activity to ensure proper D_5R signaling and, perhaps indirectly, D_1R in renal proximal tubule cells.

Previous studies showed that fenoldopam stimulation of the D_1-like dopamine receptors, specifically the D_5R, resulted in decreased AT_1R protein expression in proximal tubule cells from WKY and SHRs (14). The use of antisense oligonucleotides directed against either of the D_1-like dopamine receptors points to D_5R as the regulator of AT_1R expression (28). $D_5R^{-/-}$ knock-out mice exhibit a 30% increase in AT_1R expression compared with $D_5R^{+/+}$ wild-type littermates (14) due to decreased AT_1R degradation in the absence of D_5R (32). The increase in AT_1R expression is important in the pathogenesis and maintenance of high blood pressure in $D_5R^{-/-}$ knock-out mice because their blood pressure is normalized by systemic AT_1R blockade (32). In this study, the loss of SNX1 in hPTCs results in increased expression of both the native and glycosylated forms of AT_1R. The increase in AT_1R expression is not due to the direct interaction between SNX1 and AT_1R as these proteins do not co-immunoprecipitate in rat and human renal epithelial cells. These results indicate that the silencing of SNX1 expression leads to the impairment of D_5R function and, consequently, the up-regulation of AT_1R expression.

We silenced the expression of *Snx1* selectively in the kidneys of C56BL/6J and BALB/cJ mice as this method offers the advantage of restricted silencing of the gene of interest to relevant tissues only and precludes unforeseen compensatory mechanisms that may develop in classical systemic knock-out models. We found that renal *Snx1* silencing results in elevated systolic and diastolic blood pressures and the blunting of the natriuretic response to an agonist during salt-replete conditions, underscoring the preeminent role of the kidney in the regulation of blood pressure through the modulation of sodium transport (50). The high blood pressure of $D_5R^{-/-}$ mice is aggravated by an increase in NaCl intake (15).

Taken together, we propose that SNX1 may initiate the sorting of ligand-activated D_5R at the plasma membrane by tagging the receptor for endocytosis (Fig. 6). Alternatively, it is possible that SNX1, behaving as a peripheral membrane protein (17), may act as a scaffold or adaptor protein that facilitates the organization of D_5R, G proteins and other signaling components in phosphoinositide-enriched membrane microdomains (42, 43). The silencing of renal SNX1 impairs agonist-activated D_5R endocytosis and GTP binding, resulting in blunted cAMP response, which in turn decreases the inhibitory effects of D_5R on tubular sodium transport and increases renal sodium reabsorption (the increased sodium reabsorption is potentiated by increased tubular AT_1R expression) thus leading to sodium retention and increased blood pressure.

In summary, we have shown that D_5R and SNX1 interact in both *in vitro* and *in vivo* and that agonist treatment enhances this interaction. Inhibition of SNX1 expression or function impairs the agonist-activated D_5R internalization, prevents GTP binding, blunts the cAMP response, increases sodium transport, and up-regulates AT_1R expression. We have also shown for the first time that silencing of renal *Snx1* results in increased AT_1R expression and elevated systolic and diastolic blood pressure in two mouse strains as well as the impairment

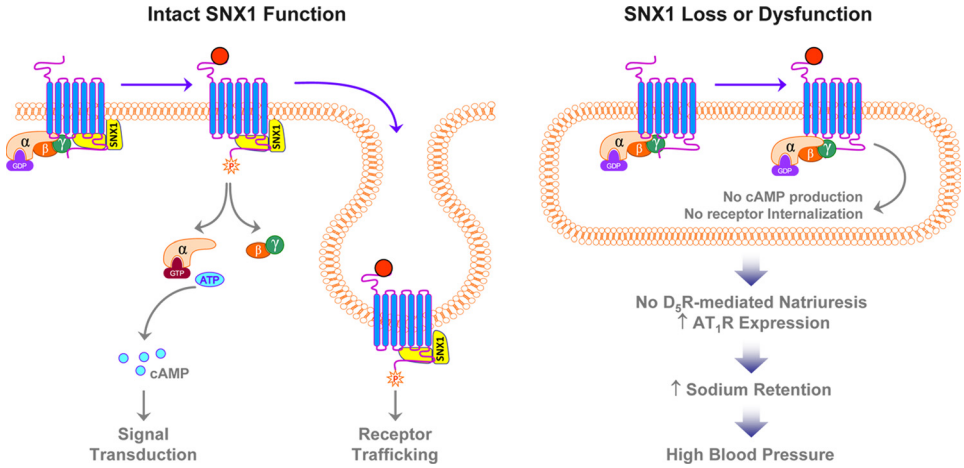

FIGURE 6. **Proposed mechanism for the SNX1 and D_5R interaction.** One of the physiological responses to moderate/high sodium intake involves the activation of the renal dopamine receptors by dopamine produced intrarenally. As with the other dopamine receptors, the occupation of the D_5R by dopamine (red dots) results in the dissociation of the cognate G protein from the receptor and its disassembly into Gα and G$\beta\gamma$ subunits after a GDP → GTP exchange at Gα. The G$\beta\gamma$ recruits a GPCR kinase that then phosphorylates the receptor. This covalent modification of the receptor prevents it from interacting with G proteins and allows it to associate with other adaptor proteins (*e.g.* β-arrestins, clathrin, and dynamin) to facilitate receptor internalization and initiate endosomal trafficking. The Gα-GTP subunit activates the adenylyl cyclase to increase cAMP levels and promote specific downstream signaling pathways, which lead to the excretion of excess sodium (natriuresis). We propose that the SNX1 may function as a scaffold or adaptor protein that facilitates the proper organization of D_5R and other membrane-bound or intracellular signaling components at the plasma membrane. SNX1 may also play a crucial role in the initial tagging of the receptor at the plasma membrane, earmarking it to a particular endosomal route. Loss or dysfunction of SNX1 results in failure of agonist-activated receptor internalization and blunting of the cAMP response to receptor activation. These in turn lead to anti-natriuresis, which is brought about by the failure of dopamine to inhibit sodium transporters and to regulate AT_1R degradation, and consequently to sodium retention and high blood pressure.

of natriuresis in response to agonist stimulation during salt-replete states. Our demonstration of deficient SNX1 expression resulting in D_5R dysfunction, increased AT_1R expression, high blood pressure, and blunted natriuretic response offers insights into a novel mechanism by which a dysfunction of a trafficking protein may consequently promote the development of hypertension.

REFERENCES

1. Jose P. A., Eisner G. M., and Felder R. A. (1998) Renal dopamine receptors in health and hypertension. *Pharmacol. Ther.* **80,** 149–182
2. Banday A. A., and Lokhandwala M. F. (2008) Dopamine receptors and hypertension. *Curr. Hypertens. Rep.* **10,** 268–275
3. Zeng C., Sanada H., Watanabe H., Eisner G. M., Felder R. A., and Jose P. A. (2004) Functional genomics of the dopaminergic system in hypertension. *Physiol. Genomics* **19,** 233–246
4. Vieira-Coelho, M. A., and Soares-da-Silva, P. (2000) Ontogenic aspects of D1 receptor coupling to G proteins and regulation of rat jejunal Na^+, K^+ ATPase activity and electrolyte transport. *Br. J. Pharmacol.* **129,** 573–581
5. Hayashi, M., Yamaji, Y., Kitajima, W., and Saruta, T. (1991) Effects of high salt intake on dopamine production in rat kidney. *Am. J. Physiol.* **260,** E675–E679
6. Siragy, H. M., Felder, R. A., Howell, N. L., Chevalier, R. L., Peach, M. J., and Carey, R. M. (1989) Evidence that intrarenal dopamine acts as a paracrine substance at the renal tubule. *Am. J. Physiol.* **257,** F469–F477
7. Felder, R. A., Seikaly, M. G., Cody, P., Eisner, G. M., and Jose, P. A. (1990) Attenuated renal response to dopaminergic drugs in spontaneously hypertensive rats. *Hypertension* **15,** 560–569
8. Sibley, D. R., and Monsma, F. J., Jr. (1992) Molecular biology of dopamine receptors. *Trends Pharmacol. Sci.* **13,** 61–69
9. Missale, C., Nash, S. R., Robinson, S. W., Jaber, M., and Caron, M. G. (1998) Dopamine receptors. From structure to function. *Physiol. Rev.* **78,** 189–225
10. Carey, R. M. (2001) Theodore Cooper lecture. Renal dopamine system. Paracrine regulator of sodium homeostasis and blood pressure. *Hypertension* **38,** 297–302
11. Rosskopf, D., Schürks, M., Rimmbach, C., and Schäfers, R. (2007) Genetics of arterial hypertension and hypotension. *Naunyn Schmiedebergs Arch. Pharmacol.* **374,** 429–469
12. Hollon, T. R., Bek, M. J., Lachowicz, J. E., Ariano, M. A., Mezey, E., Ramachandran, R., Wersinger, S. R., Soares-da-Silva, P., Liu, Z. F., Grinberg, A., Drago, J., Young, W. S., 3rd, Westphal, H., Jose, P. A., and Sibley, D. R. (2002) Mice lacking D5 dopamine receptors have increased sympathetic tone and are hypertensive. *J Neurosci.* **22,** 10801–10810
13. Yang, Z., Asico, L. D., Yu, P., Wang, Z., Jones, J. E., Escano, C. S., Wang, X., Quinn, M. T., Sibley, D. R., Romero, G. G., Felder, R. A., and Jose, P. A. (2006) D5 dopamine receptor regulation of reactive oxygen species production, NADPH oxidase, and blood pressure. *Am. J. Physiol. Regul. Integr. Comp. Physiol.* **290,** R96–R104
14. Zeng, C., Yang, Z., Wang, Z., Jones, J., Wang, X., Altea, J., Mangrum, A. J., Hopfer, U., Sibley, D. R., Eisner, G. M., Felder, R. A., and Jose, P. A. (2005) Interaction of angiotensin II type 1 and D5 dopamine receptors in renal proximal tubule cells. *Hypertension.* **45,** 804–810
15. Yang Z., Sibley D.R., and Jose P.A. (2004) D5 dopamine receptor knockout mice and hypertension. *J. Recept. Signal. Transduct. Res.* **24,** 149–164
16. Thompson, D., and Whistler, J. L. (2011) Trafficking properties of the D5 dopamine receptor. *Traffic* **12,** 644–656
17. Haft, C. R., de la Luz Sierra, M., Barr, V. A., Haft, D. H., and Taylor, S. I. (1998) Identification of a family of sorting nexin molecules and characterization of their association with receptors. *Mol. Cell. Biol.* **18,** 7278–7287
18. Heydorn, A., Søndergaard, B. P., Hadrup, N., Holst, B., Haft, C. R., and Schwartz, T. W. (2004) Distinct *in vitro* interaction pattern of dopamine receptor subtypes with adaptor proteins involved in post-endocytotic receptor targeting. *FEBS Lett.* **556,** 276–280
19. Ponting, C. P. (1996) Novel domains in NADPH oxidase subunits, sorting nexins, and PtdIns 3-kinases. Binding partners of SH3 domains? *Protein Sci.* **5,** 2353–2357
20. Worby C.A., and Dixon J.E. (2002) Sorting out the cellular functions of sorting nexins. *Nat. Rev. Mol. Cell Biol.* **3,** 919–931
21. Hierro, A., Rojas, A. L., Rojas, R., Murthy, N., Effantin, G., Kajava, A. V., Steven, A. C., Bonifacino, J. S., and Hurley, J. H. (2007) Functional architecture of the retromer cargo-recognition complex. *Nature* **449,** 1063–1067
22. Kurten, R. C., Cadena, D. L., and Gill, G. N. (1996) Enhanced degradation of EGF receptors by a sorting nexin, SNX1. *Science* **272,** 1008–1010
23. Pons, V., Hullin-Matsuda, F., Nauze, M., Barbaras, R., Pérès, C., Collet, X.,

Perret, B., Chap, H., and Gassama-Diagne, A. (2003) Enterophilin-1, a new partner of sorting nexin 1, decreases cell surface epidermal growth factor receptor. *J. Biol. Chem.* **278,** 21155–21161
24. Mari, M., Bujny, M. V., Zeuschner, D., Geerts, W. J., Griffith, J., Petersen, C. M., Cullen P. J., Klumperman, J., and Geuze, H. J. (2008) SNX1 defines an early endosomal recycling exit for sortilin and mannose 6-phosphate receptors. *Traffic* **9,** 380–393
25. Wang, Y., Zhou, Y., Szabo, K., Haft, C. R., and Trejo, J. (2002) Down-regulation of protease-activated receptor-1 is regulated by sorting nexin 1. *Mol. Biol. Cell* **13,** 1965–1976
26. Prosser, D. C., Tran, D., Schooley, A., Wendland, B., and Ngsee, J. K. (2010) A novel, retromer-independent role for sorting nexins 1 and 2 in RhoG-dependent membrane remodeling. *Traffic* **11,** 1347–1362
27. Nisar, S., Kelly, E., Cullen, P. J., and Mundell, S. J. (2010) Regulation of P2Y1 receptor traffic by sorting Nexin 1 is retromer independent. *Traffic* **11,** 508–519
28. Gildea, J. J., Wang, X., Jose, P. A., and Felder, R. A. (2008) Differential D1 and D5 receptor regulation and degradation of the angiotensin type 1 receptor. *Hypertension* **51,** 360–366
29. Felder, R. A., Sanada, H., Xu, J., Yu, P. Y., Wang Z., Watanabe, H., Asico, L. D., Wang, W., Zheng, S., Yamaguchi, I., Williams, S. M., Gainer, J., Brown, N. J., Hazen-Martin, D., Wong, L. J., Robillard, J. E., Carey, R. M., Eisner, G. M., and Jose, P. A. (2002) G protein-coupled receptor kinase 4 gene variants in human essential hypertension. *Proc. Natl. Acad. Sci. U.S.A.* **99,** 3872–3877
30. Yu, P., Asico, L. D., Luo, Y., Andrews, P., Eisner, G. M., Hopfer, U., Felder, R. A., and Jose, P. A. (2006) D1 dopamine receptor hyperphosphorylation in renal proximal tubules in hypertension. *Kidney Int.* **70,** 1072–1079
31. Chen Y., Elangovan M., and Periasamy A. (2005) *Molecular Imaging: FRET Microscopy and Spectroscopy,* 1st Ed., pp. 126–135, Oxford University Press, New York
32. Li, H., Armando, I., Yu, P., Escano, C., Mueller, S. C., Asico, L., Pascua, A., Lu, Q., Wang, X., Villar, V. A., Jones, J. E., Wang, Z., Periasamy, A., Lau, Y. S., Soares-da-Silva, P., Creswell, K., Guillemette, G., Sibley, D. R., Eisner, G., Gildea, J. J., Felder, R. A., and Jose, P. A. (2008) Dopamine 5 receptor mediates Ang II type 1 receptor degradation via a ubiquitin-proteasome pathway in mice and human cells. *J. Clin. Invest.* **118,** 2180–2189
33. Escano, C. S., Armando, I., Wang, X., Asico, L. D., Pascua, A., Yang, Y., Wang, Z., Lau, Y. S., and Jose P. A. (2009) Renal dopaminergic defect in C57Bl/6J mice. *Am. J. Physiol. Regul. Integr. Comp. Physiol.* **297,** R1660–R1669
34. Schwarz, D. G., Griffin, C. T., Schneider, E. A., Yee, D., and Magnuson, T. (2002) Genetic analysis of sorting nexins 1 and 2 reveals a redundant and essential function in mice. *Mol. Biol. Cell* **13,** 3588–3600
35. Guo, Y., and Jose, P. A. (2011) C-terminal dileucine motif of dopamine D receptor plays an important role in its plasma membrane trafficking. *PLoS One* **6,** e29204
36. Yao, L. P., Li, X. X., Yu, P. Y., Xu, J., Asico, L. D., Jose, P. A. (1998) Dopamine D1 receptor and protein kinase C isoforms in spontaneously hypertensive rats. *Hypertension* **32,** 1049–1053
37. Christie, M. I., Harper, D., Smith G.W. (1992) Analysis of the agonist activity of fenoldopam (SKF 82526) at the vascular 5-HT2 receptor. *Br. J. Pharmacol.* **107,** 1008–1012
38. Brismar, H., Asghar, M., Carey, R. M., Greengard, P., and Aperia, A. (1998) Dopamine-induced recruitment of dopamine D1 receptors to the plasma membrane. *Proc. Natl. Acad. Sci. U.S.A.* **95,** 5573–5578
39. He, Y., Yu, L. P., and Jin, G. Z. (2009) Differential distributions and trafficking properties of dopamine D1 and D5 receptors in nerve cells. *Neurosci Bull.* **25,** 43–53
40. Tiberi, M., and Caron, M. G. (1994) High agonist-independent activity is a distinguishing feature of the dopamine D1B receptor subtype. *J. Biol. Chem.* **269,** 27925–27931
41. Carlton, J., Bujny, M., Rutherford, A., and Cullen P. (2005) Sorting nexins. Unifying trends and new perspectives. *Traffic* **6,** 75–82
42. Hanyaloglu, A. C., and von Zastrow, M. (2008) Regulation of GPCRs by endocytic membrane trafficking and its potential implications. *Annu. Rev. Pharmacol. Toxicol.* **48,** 537–568
43. Clague M.J., and Urbé S. (2001) The interface of receptor trafficking and signalling. *J. Cell Sci.* **114,** 3075–3081
44. Wang, X., Villar, V. A., Armando, I., Eisner, G. M., Felder, R. A., and Jose, P. A. (2008) Dopamine, kidney, and hypertension. Studies in dopamine receptor knockout mice. *Pediatr. Nephrol.* **23,** 2131–2146
45. Calebiro, D., Nikolaev, V. O., Persani, L., and Lohse, M. J. (2010) Signaling by internalized G-protein-coupled receptors. *Trends Pharmacol. Sci.* **31,** 221–228
46. Yu, P., Asico, L. D., Eisner, G. M., Hopfer, U., Felder, R. A., and Jose, P. A. (2000) Renal protein phosphatase 2A activity and spontaneous hypertension in rats. *Hypertension* **36,** 1053–1058
47. Ferrandon, S., Feinstein, T. N., Castro, M., Wang, B., Bouley, R., Potts, J. T., Gardella, T. J., and Vilardaga, J. P. (2009) Sustained cyclic AMP production by parathyroid hormone receptor endocytosis. *Nat. Chem. Biol.* **5,** 734–742
48. Mullershausen, F., Zecri, F., Cetin, C., Billich, A., Guerini, D., and Seuwen, K. (2009) Persistent signaling induced by FTY720-phosphate is mediated by internalized S1P1 receptors. *Nat. Chem. Biol.* **5,** 428–434
49. Calebiro, D., Nikolaev, V. O., Gagliani, M. C., de Filippis T., Dees, C., Tacchetti, C., Persani, L., and Lohse, M. J. (2009) Persistent cAMP-signals triggered by internalized G-protein-coupled receptors. *PLoS Biol.* **7,** e1000172
50. Crowley, S. D., and Coffman, T. M. (2007) In hypertension, the kidney rules. *Curr. Hypertens. Rep.* **9,** 148–153